

International Conference on Computational Heat and Mass Transfer-2015

## Heat Transfer and Fluid Flow Characteristics from Finite Height Circular Cylinder Mounted on Horizontal Plate

Hemant Naik<sup>\*</sup>, Shaligram Tiwari

*Department of Mechanical Engineering, IIT Madras, Chennai, 600036, India*

---

### Abstract

Present study deals with three-dimensional numerical investigations of flow and heat transfer characteristics around a finite height circular cylinder mounted on a horizontal plate. Uniform flow has been assumed at the inlet which develops and flows across the cylinder. Flow separation has been observed from the leading edge of free-end of the cylinder, sides of the cylinder and in upstream nearer to the cylinder just above the bottom plate. Cylinder and bottom plate are maintained at constant temperature which is higher than the free stream temperature of the fluid. The study has been carried out for a cylinder with aspect ratio (ratio of height to diameter) of 3 and Reynolds number (Re) in the range of 40 to 100. Detailed flow patterns have been presented in the form of time-averaged streamlines in different planes. Temperature and Nusselt number contours have also been presented near the bottom plate. In addition, variation of perimeter-averaged Nusselt number along the height of the cylinder and variation of height-averaged Nusselt number around the cylinder have been presented.

© 2015 The Authors. Published by Elsevier Ltd. This is an open access article under the CC BY-NC-ND license (<http://creativecommons.org/licenses/by-nc-nd/4.0/>).

Peer-review under responsibility of the organizing committee of ICCHMT – 2015

*Keywords:* Flow separation; finite circular cylinder; perimeter-averaged Nusselt number; height-averaged Nusselt number.

---

### 1. Introduction

Flow and heat transfer past a finite height circular cylinder mounted on a horizontal plate have been a common topic of research for many years. The study is of much practical importance in various engineering fields, such as heat exchangers, cooling towers, chimneys, etc. Various topological flow fields develop around the cylinder which can affect the heat transfer greatly. Such a flow field can be used for cooling of electronic devices by heat transfer

---

<sup>\*</sup> Corresponding author. Tel.: 08939079004.  
E-mail address: [me14d014@iitm.ac.in](mailto:me14d014@iitm.ac.in)

enhancement. [1] presented the effect of heat transfer from a finite height circular cylinder mounted on a plate for aspect ratio (AR) in the range from 1 to 6. It has been reported that heat transfer characteristics depend on AR, boundary layer thickness and nature of the flow field. Comparison of various local and peripheral averaged heat transfer coefficients of a finite circular cylinder with the two-dimensional cylinder have also been presented. Effect of heat transfer on flow separation and reattachment has been discussed by [2] and [3]. The horseshoe vortex plays a dominant role in heat transfer from the side surface of the cylinder. Higher heat transfer has been reported just below the leading edge in downstream for low values of AR. A brief review of flow field with and without heat transfer has been given by [4] for flow above free-end of the plate mounted cylinder.

Ghisalberti [5] reported the effects of flow on heat transfer around bodies of various shapes like circular cylinder, cone, square bar, etc. They also reported that heat transfer enhancement depends on AR of the cylinder. Numerical investigation has been carried out by [6] to understand the flow structure and heat transfer rate from circular tube at moderate values of Reynolds number (Re). Experimental investigation has been carried out by [7] for flow past circular cylinder fixed between two parallel plates. Horseshoe vortices formed around the cylinder wall junction increase the heat transfer rate. Influence of AR on flow field has been reported by [8] for different values of AR (3, 5, 7 and 9). In downstream just behind the cylinder, a large recirculation region and a small vortex nearer to the free end has been observed for all four AR values considered and a second vortex is observed in downstream near the cylinder-bottom wall junction only for AR values of 5, 7 and 9.

The main objective of present study is to identify the flow and heat transfer characteristics around the finite circular cylinder of AR equal to 3 at Re values of 40, 60 and 100. Investigations of flow and heat transfer characteristics from the heated cylinder and bottom wall have been carried out with the help of streamline plots and temperature contours. By the comparison of perimeter-averaged Nusselt number along the cylinder height and height-averaged Nusselt number along the periphery of the cylinder, region of higher heat transfer can be identified.

## 2. Problem Statement

The computational domain for the present study has been shown in Fig. 1. The domain of interest consists of a finite circular cylinder of diameter ' $d$ ' and height ' $H$ ' mounted on a horizontal plate. The surfaces of the cylinder and bottom plate are maintained at a constant temperature ' $T_w$ ' which is greater than the free stream temperature ( $T_\infty$ ). The dimensions of the computational domain are fixed as length ( $L_1$ ) =  $30d$ , width ( $L_2$ ) =  $10d$  and height ( $L_3$ ) =  $7d$ . The cylinder is placed at a distance of  $10d$  from the inlet. The AR value for the cylinder has been fixed as 3 and computations have been carried out for Re values in the range of 40 to 100. The velocity and temperature profiles are assumed to be uniform at the inlet. In Fig. 1, inlet face, outlet face, bottom wall and cylinder can be identified clearly. Surface parallel to the bottom wall and above the cylinder is top wall and surfaces perpendicular to the bottom wall are side walls of the computational domain.

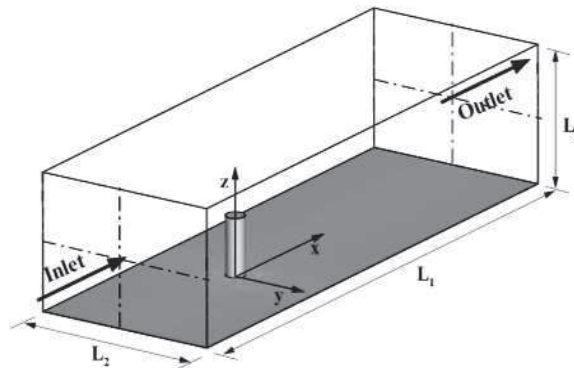


Fig. 1. Computational domain

### 3. Governing Equations and Boundary Conditions

#### 3.1 Governing Equations

In a Cartesian coordinate system, the dimensionless governing equations for the three-dimensional, laminar, incompressible flow and heat transfer with constant thermos-physical properties and negligible dissipation effect can be expressed in the tensor form as given below.

Continuity equation

$$\frac{\partial u_i}{\partial x_i} = 0 \quad (1)$$

Momentum equation

$$\frac{\partial u_i}{\partial t} + \frac{\partial(u_i u_j)}{\partial x_j} = -\frac{\partial p}{\partial x_i} + \frac{1}{\text{Re}} \left( \frac{\partial^2 u_i}{\partial x_j \partial x_j} \right) \quad (2)$$

Energy equation

$$\frac{\partial \theta}{\partial t} + \frac{\partial(u_j \theta)}{\partial x_j} = \frac{1}{\text{Re Pr}} \left( \frac{\partial^2 \theta}{\partial x_j \partial x_j} \right) \quad (3)$$

where  $\text{Re} = U_\infty d/\nu$  and non-dimensionalized temperature  $\theta = (T - T_\infty)/(T_w - T_\infty)$ .

Here  $u_i$  is the dimensionless velocity component along  $x_i$  coordinate direction. For a 3-D coordinate system, Equation (2) collectively represents the  $x$ ,  $y$  and  $z$ -components of the momentum equation for values of  $x_i$  as  $x$ ,  $y$  and  $z$  and  $u_i$  as  $u$ ,  $v$  and  $w$  respectively. Also  $p$  is the dimensionless pressure,  $t$  is dimensionless time,  $\text{Re}$  is Reynolds number,  $\text{Pr}$  is Prandtl number,  $U_\infty$  is free-stream velocity,  $\nu$  is the kinematic viscosity,  $\theta$  is the dimensionless temperature. Moreover,  $T_\infty$  is free-stream temperature and  $T_w$  is wall temperature of cylinder and bottom plate. The pressure has been non-dimensionalized by  $\rho U_\infty^2$  while temperature by  $(T_w - T_\infty)$ .

#### 3.2 Boundary Conditions

The boundary conditions imposed at the inlet, outlet, cylinder surface and different walls of the domain are given below;

*Inlet:* Uniform velocity,  $(u = U_\infty, v = w = 0, T = T_\infty)$

*Outlet:* Pressure outlet,  $(p = p_\infty)$

*Side walls:* Free-slip boundaries,  $(v = 0, \frac{\partial u}{\partial y} = \frac{\partial w}{\partial y} = \frac{\partial p}{\partial y} = \frac{\partial T}{\partial y} = 0)$

*Top wall:* Free-slip boundaries,  $(w = 0, \frac{\partial u}{\partial z} = \frac{\partial v}{\partial z} = \frac{\partial p}{\partial z} = \frac{\partial T}{\partial z} = 0)$

*Cylinder surfaces and bottom wall:* No-slip and isothermal boundaries,  $(u = v = w = 0, T = T_w)$

### 4. Numerical Technique and Grid Independence Study

#### 4.1 Numerical Technique

Finite volume based commercial software ANSYS Fluent 14.0 has been used for the present computations. The

governing equations have been solved using finite volume discretization based SIMPLE (Semi Implicit Method for Pressure Linked Equations) algorithm. First order accurate implicit scheme has been used for transient formulation and second order upwind scheme has been used for discretizing the convective terms.

#### 4.2 The Grid and Grid Independence Study

The grid used for computations is non-uniform structured hexahedral mesh, which is created by using commercial software ANSYS ICEM 14. The O-type grid structure is created close to the cylinder and hexahedral structure everywhere else in the domain. The schematic of the grid used for the present computations is shown in Fig 2. In numerical computations, it becomes essential to perform a grid independence study. In the present work, the grid independence is achieved by carrying out computations using four different grid sizes for same domain size and the details are given in Table-1 below. The number of cells in whole computation domain, the number of grid points on the circumference of the cylinder and mean drag coefficient are shown in Table-1. From the results of Table-1, it is confirmed that for 120 grid points on the cylinder surface, the change in computed values is much less significant. Accordingly, all the computations have been carried out for a grid size that corresponds to 120 divisions on the cylinder surface.

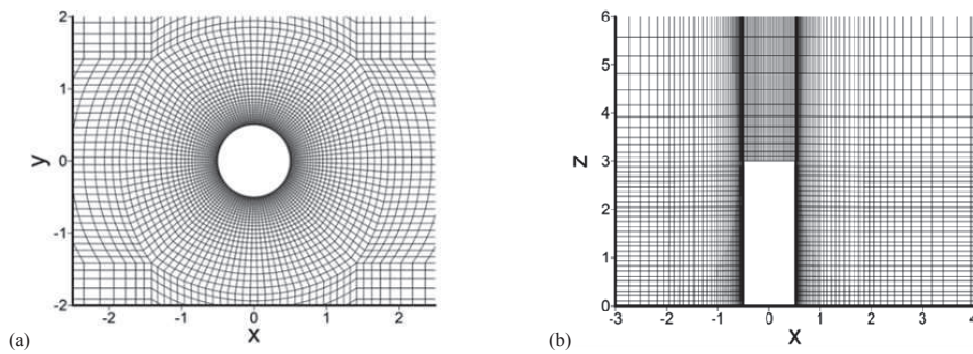


Fig. 2. Schematic of grid (a) plane view parallel to bottom wall at  $z = 1.0$  (b) plane view parallel to side wall at  $y = 0$

Table 1. Comparison of mean drag coefficient for different grids at  $Re = 100$ .

No. of cells	No. of grid points on cylinders	$Cd_{mean}$
295875	80	1.1294
320815	100	1.1315
345755	120	1.1324
395635	160	1.1325

## 5. Results and Discussion

### 5.1 Time-averaged Flow Characteristics

Figure 3 shows the time-averaged streamlines in different vertical planes along the wake for different values of  $Re$ . It has been observed that in the upstream of the cylinder, some part of the flow moves upward and some part of the flow moves downward. Flow separation takes place from the leading edge of the cylinder's free-end for the flow which moves upward. For the flow which moves downward, separation takes place in two regions, one in front of the cylinder and nearer to the bottom plate while the other from the side surface of the cylinder. Figure 3 also shows that in the downstream of the cylinder, just below the free end, vortex formation takes place. It is observed that with increase in the value of  $Re$ , the size of vortex also increases. As one moves from centre plane ( $y = 0$ ) towards side wall of the domain, the size of vortex decreases and slowly it gets eliminated. Reattachment saddle has been noticed in downstream of the cylinder corresponding to this vortex. The saddle point observed in  $x$ - $z$  plane at  $y = 0$  moves along the flow direction as  $Re$  increases. For  $Re$  equal to 100, an additional vortex is formed in the downstream just

behind the cylinder and below the main vortex.

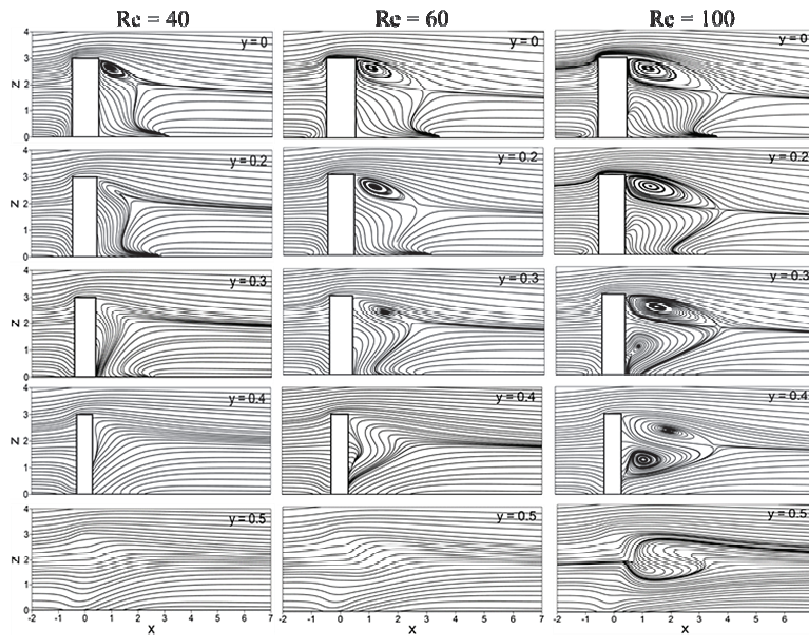


Fig. 3. Time-averaged streamlines in different  $x$ - $z$  planes

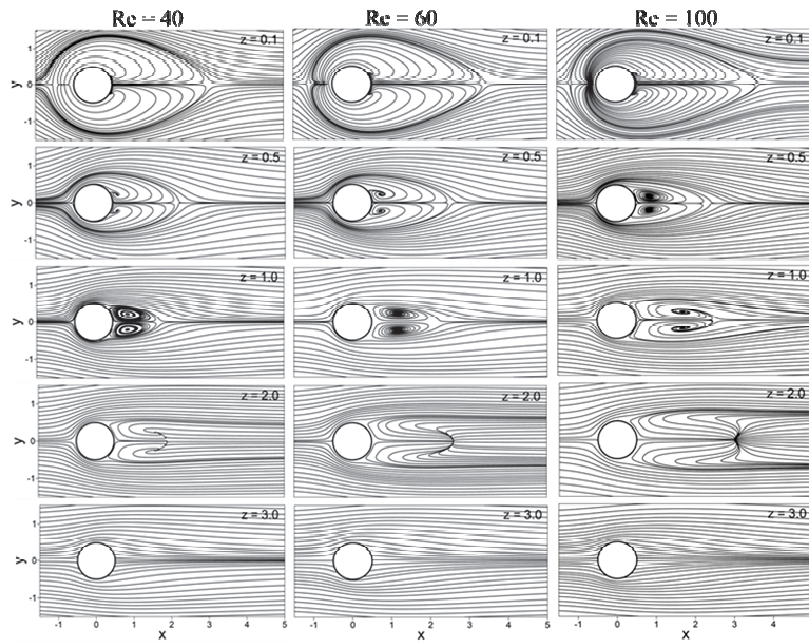


Fig. 4. Time-averaged streamlines in different  $x$ - $y$  planes



Figure 4 shows the time-averaged streamlines in different horizontal planes for different values of  $Re$ . A symmetrical flow behaviour can be seen on both the sides from centreline along the flow direction. For  $z = 0.1$ , separation saddle has been observed in upstream of the cylinder. It is also observed that flow has two recirculation zones behind the cylinder which reattach at the 'attachment saddle'. As the value of  $Re$  increases, the size of this recirculation zone also increases. As we move upwards from the bottom wall, this recirculation zone decreases in size and at top of the cylinder it gets completely eliminated.

## 5.2 Time-averaged Heat Transfer Characteristics

### 5.2.1 Nusselt number

Nusselt number ( $Nu$ ) contour near the bottom wall for different values of  $Re$  has been shown in Fig. 5. In the wake region the value of  $Nu$  is lower as compared to that in other regions. It has been observed that as value of  $Re$  increases, value of Nusselt number also increases.

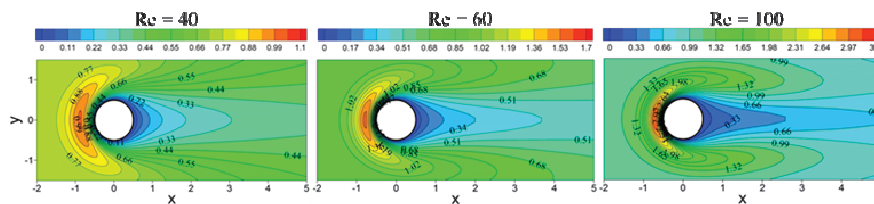


Fig. 5. Contours of Nusselt number near the bottom plate for different values of  $Re$

Figure 6(a) shows the variation of perimeter-averaged Nusselt number along the height of the cylinder. It has been observed that as height increases, the perimeter-averaged Nusselt number also increases. For cylinder height from  $z = 0$  to  $0.5$  and  $z = 2.5$  to  $3.0$ , there is sudden increase in the value of perimeter-averaged Nusselt number and in between  $z = 0.5$  to  $2.5$  gradual increase is observed. Higher value of perimeter-averaged Nusselt number is found for higher value of  $Re$  at every location. Figure 6 (b) shows the variation of height-averaged Nusselt number along the perimeter of the cylinder. From upstream to downstream along the periphery of the cylinder, height-averaged Nusselt number decreases. Higher value of height-averaged Nusselt number is found for higher value of  $Re$  at every  $\theta$ -location.

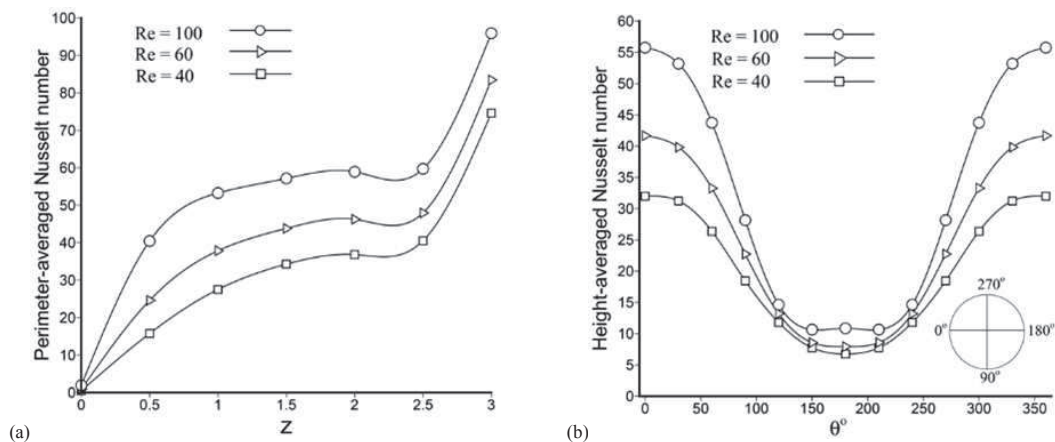


Fig. 6. Variation of (a) perimeter-averaged Nusselt number along the height of cylinder (b) height- averaged Nusselt number along the perimeter of cylinder

### 5.2.2 Temperature contours

Contours of temperature in different horizontal planes for different values of  $Re$  have been shown in Fig. 7. The temperature difference between cylinder wall and fluid in the wake has been found to be small while more temperature difference is observed between fluid in upstream and the cylinder wall. As the value of  $Re$  increases, there occurs an increase in temperature difference between cylinder wall and the fluid in the wake while less increase in the temperature difference has been found between the temperature of fluid in upstream and the cylinder wall.

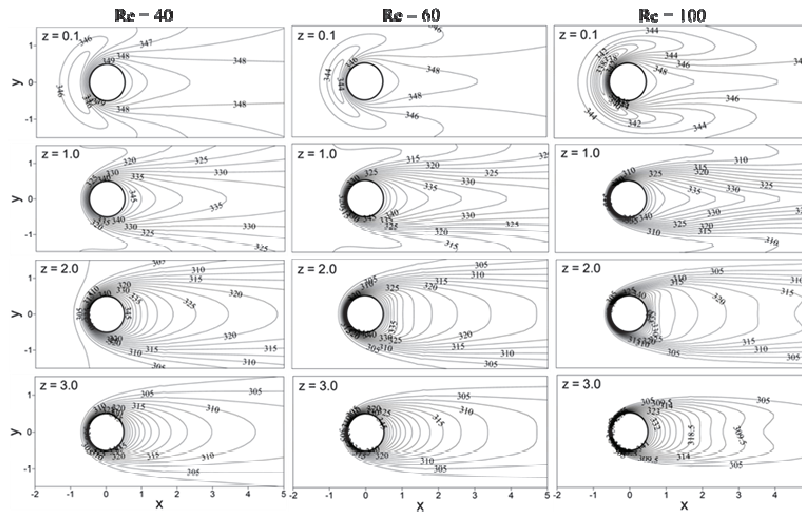


Fig. 7. Contours of temperature in different horizontal planes for different values of  $Re$

Figure 8 shows the contours of temperature in different vertical planes along the flow direction for different values of  $Re$ . In upstream and downstream nearer to the cylinder surface as well as bottom surface, fluid has higher value of temperature, but at the top of the cylinder surface it has relatively lower value. The fluid temperature is higher in upstream and downstream of the cylinder and as we move from  $y = 0$  to side wall of the domain, the value of fluid temperature decreases. Both in upstream and downstream of the cylinder, as value of  $Re$  increases, the temperature difference between the bottom wall and the fluids also increases.

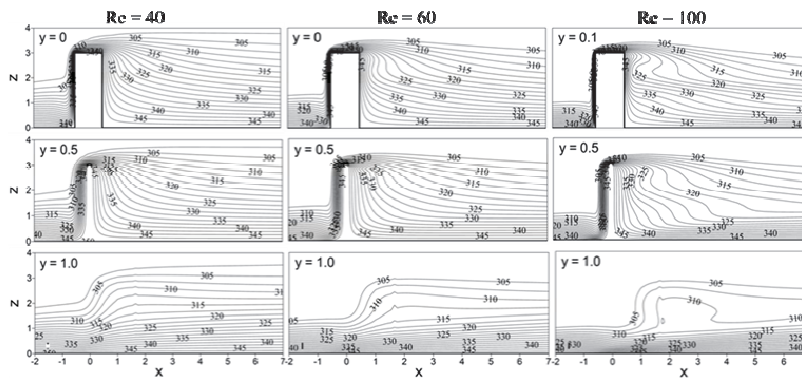


Fig. 8. Contours of temperature in different  $x$ - $z$  planes for different values of  $Re$

## 6. Conclusion

Fluid flow and heat transfer characteristics around a finite height circular cylinder mounted on a horizontal plate have been investigated. For a finite cylinder of height  $3d$  and Reynolds number in the range of 40 to 100, three-dimensional numerical simulations have been carried out. Wake patterns are highly dependent on the value of  $Re$  and  $AR$ . As the value of  $Re$  increases wake length also increases. Flow separation region in the upstream nearer to the cylinder just above the bottom plate is the region where horseshoe vortex formation takes place. Reattachment region has been found in the downstream and the distance between the cylinder and this region increases as value of  $Re$  increases. Heat transfer from the heated cylinder and bottom wall to the fluid is more for higher value of  $Re$ . Perimeter-averaged Nusselt number is more on the top of the cylinder and less at the bottom of the cylinder. Height-averaged Nusselt number is higher near front and lower at near rear stagnation lines. Higher temperature difference has been observed in the wake for higher values of  $Re$ .

## References

- [1] T. Kawamura, M. Hiwada, T. Hibino, T. Mabuchi and M. Kumada, Heat transfer from a finite circular cylinder on the flat plate, *Bulletin of the JSME* 27 (1984) 2430–2439
- [2] T. Tsutsui, T. Igarashi and H. Nakamura, Fluid flow and heat transfer around a cylindrical protuberance mounted on a flat plate boundary layer, *JSME International Journal* 43 (2000) 279–287.
- [3] T. Tsutsui and M. Kawahara, Heat transfer around a cylindrical protuberance mounted in a plane turbulent boundary layer, *ASME Journal of Heat Transfer* 128 (2006) 153–161.
- [4] D. Sumner, Flow above the free end of a surface-mounted finite-height circular cylinder: A review, *Journal of Fluids and Structures* 43 (2013) 41–63.
- [5] L. Ghisalberti, A. Kondjoyan, Convective heat transfer coefficients between air flow and a short cylinder, Effect of air velocity and turbulence, Effect of body shape, dimensions and position in the flow, *Journal of Food Engineering* 42 (1999) 33–44.
- [6] S. Tiwari, G. Biswas, P.L.N. Prasad and B. Sudipta, Numerical prediction of flow and heat transfer in a rectangular channel with a built-in circular tube, *Journal of Heat Transfer (ASME)* 125 (2003) 413–421.
- [7] B. Sahin, N.A. Ozturk and C. Gurlek, Horseshoe vortex studies in the passage of a model plate-fin-and-tube heat exchanger, *International Journal of Heat and Fluid Flow* 29 (2008) 340–351.
- [8] N. Rostamy, D. Sumner, D.J. Bergstrom and J.D. Bugg, Local flow field of a surface-mounted finite circular cylinder, *Journal of Fluids and Structures* 34 (2012) 105–122.